Article

Nitrosonium-Catalyzed Decomposition of *S*-Nitrosothiols in Solution: A Theoretical and Experimental Study

Yi-Lei Zhao, Patrick R. McCarren, K. N. Houk, Bo Yoon Choi, and Eric J. Toone

J. Am. Chem. Soc., **2005**, 127 (31), 10917-10924• DOI: 10.1021/ja050018f • Publication Date (Web): 15 July 2005

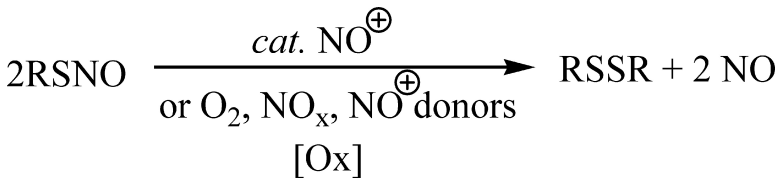

More About This Article

Additional resources and features associated with this article are available within the HTML version:

- Supporting Information
- Links to the 4 articles that cite this article, as of the time of this article download
- Access to high resolution figures
- Links to articles and content related to this article
- Copyright permission to reproduce figures and/or text from this article

View the Full Text HTML

J|A|C|S
ARTICLES
Published on Web 07/15/2005

Nitrosonium-Catalyzed Decomposition of *S*-Nitrosothiols in Solution: A Theoretical and Experimental Study

Yi-Lei Zhao,[†] Patrick R. McCarren,[†] K. N. Houk,*[,†] Bo Yoon Choi,[‡] and Eric J. Toone*[,‡]

Contribution from the Department of Chemistry and Biochemistry, University of California, Los Angeles, California 90095-1569, and Department of Chemistry and Biochemistry, Duke University, Durham, North Carolina 27708

Received January 3, 2005; E-mail: houk@chem.ucla.edu; eric.toone@duke.edu

Abstract: The decomposition of *S*-nitrosothiols (RSNO) in solution under oxidative conditions is significantly faster than can be accounted for by homolysis of the S−N bond. Here we propose a cationic chain mechanism in which nitrosation of nitrosothiol produces a nitrosated cation that, in turn, reacts with a second nitrosothiol to produce nitrosated disulfide and the NO dimer. The nitrosated disulfide acts as a source of nitrosonium for nitrosothiol nitrosation, completing the catalytic cycle. The mechanism accounts for several unexplained facets of nitrosothiol chemistry in solution, including the observation that the decomposition of an RSNO is accelerated by O_2, mixtures of O_2 and NO, and other oxidants, that decomposition is inhibited by thiols and other antioxidants, that decomposition is dependent on sulfur substitution, and that decomposition often shows nonintegral kinetic orders.

Introduction

Nitric oxide is an ubiquitous biological species with myriad activities. Although nitric oxide is synthesized enzymatically as the neutral +2 oxide of nitrogen, several other nitrogen oxides, including the +3 (NO^+) and +1 (NO^-/HNO) oxides, are known and have been implicated in various biological processes. The +3 oxide exists in vivo primarily as *S*-nitrosothiol (RSNO); these species, especially *S*-nitrosoglutathione, represent the largest circulating pool of nitric oxide.[1] *S*-Nitrosation of protein thiols may also represent an important post-translational modification involved in both regulation and signaling.

S-Nitrosothiols are typically regarded as unstable in solution, and under some conditions many decompose with half-lives of seconds to minutes.[2] Although primary and secondary *S*-nitrosothiols are often regarded as less stable than the corresponding tertiary compounds, wide variations in stability are the rule and conflicting values are often reported.[3] The time course of *S*-nitrosothiol decomposition is complex and frequently shows nonintegral kinetic orders.[4]

S-Nitrosothiol decomposition produces a range of organic and inorganic products, but in many cases decomposition liberates neutral nitric oxide and disulfide. Activation energies for the decomposition of *S*-nitrosothiol have been reported from 20 to 31 kcal mol^{-1} by different groups.[5,6] Although NO is formally the product of S−N bond scission, homolytic bond dissociation energies for variously substituted alkyl *S*-nitrosothiols in the gas phase are uniformly near 31 kcal mol^{-1}, values that predict apparent half-lives of years near room temperature.[6] Additionally, the uniformity of bond dissociation energies as a function of sulfur substitution is inconsistent with frequently observed variation in nitrosothiol stability as a function of substitution. Accordingly, we continue our efforts to elucidate important pathways of nitrosothiol decomposition.

The stability of *S*-nitrosothiols is highly dependent on reaction conditions. A reductive decomposition mediated by cuprous ion has been well established by Williams and co-workers.[7] Oxidative conditions are also known to induce *S*-nitrosothiol decomposition, and Grossi et al. recently proposed a catalytic

[†] University of California.
[‡] Duke University.

(1) (a) Stamler, J. S. *Cell* **1994**, *78*, 931−936. (b) Stamler, J. S. *Curr. Top. Microbiol. Immunol.* **1995**, *196*, 19−36. (c) Williams, D. L. H. *Acc. Chem. Res.* **1999**, *32*, 869−876.
(2) (a) Singh, S. P.; Wishnok, J. S.; Sechive, M.; Deen, W. M.; Tannenbaum, S. R. *Proc. Natl. Acad. Sci. U.S.A.* **1996**, *93*, 14428−14433. (b) Munro, A. P.; Williams, D. L. H. *Can. J. Chem.* **1999**, *77*, 550−556. (c) Singh, R. J.; Hogg, N.; Joseph, J.; Kalyanaraman, B. *J. Biol. Chem.* **1996**, *271*, 18596−18603.
(3) (a) Oae, E.; Fukushima, D.; Kim, Y. H. *J. Chem. Soc., Chem. Commun.* **1977**, 407−408. (b) Ignarro, L. J.; Lippton, H.; Edwards, J. C.; Baricos, W. H.; Hymann, A. L.; Kadowitz, P. J.; Gruetter, C. A. *J. Pharmacol. Exp. Ther.* **1981**, *218*, 739−749.
(4) De Oliveria, M. G.; Shishido, S. M.; Seabra, A. B.; Morgon, N. H. *J. Phys. Chem. A* **2002**, *106*, 8963−8970 and references therein.
(5) The BDE of tertiary RSNO is somewhat lower than that of primary RSNO; thermal decomposition of tertiary RSNO is faster than that of primary RSNO. (a) Grossi, L.; Montevecchi, P. C. *Chem.—Eur. J.* **2002**, *8*, 380−387. (b) Lu, J.-M.; Wittbrodt, J. M.; Wang, K.; Wen, Z.; Schlegel, H. B.; Wang, P. G.; Cheng, J.-P. *J. Am. Chem. Soc.* **2001**, *123*, 2903−2904.
(6) (a) Bartberger, M. D.; Mannion, J. D.; Powell, S. C.; Stamler, J. S.; Houk, K. N.; Toone, E. J. *J. Am. Chem. Soc.* **2001**, *123*, 8868−8869. (b) Bartberger, M. D.; Houk, K. N.; Power, S. C.; Mannion, J. D.; Lo, K. Y.; Stamler, J. S.; Toone, E. J. *J. Am. Chem. Soc.* **2000**, *122*, 5889−5890. (c) Baciu, C.; Gauld, J. W. *J. Phys. Chem. A* **2003**, *107*, 9946−9952.
(7) (a) Williams, D. L. H. *Chem. Commun.* **1996**, 1085−1090. (b) Dicks, A. P.; Swift, H. R.; Williams, D. L. H.; Butler, A. R.; Al-S'adoni, H. H.; Cox, B. G. *J. Chem. Soc., Perkin Trans. 2* **1996**, 481−487. (c) Stubauer, G.; Giuffre, A.; Sarti, P. *J. Biol. Chem.* **1999**, *274*, 28128−28133. (d) Ramirez, J.; Yu, L.; Li, J.; Braunschweiger, P. G.; Wang, P. G. *Bioorg. Med. Chem. Lett.* **1996**, *6* (21), 2575−2580. (e) Megson, I. L.; Greig, I. R.; Gray, G. A.; Webb, D. J.; Butler, A. R. *Br. J. Pharmacol.* **1997**, *122* (8), 1617−1624.

10.1021/ja050018f CCC: $30.25

decomposition pathway initiated by nitrosothiol homolysis and mediated by N_2O_3.[8]

Here we report theoretical and experimental studies on a catalytic decomposition pathway for nitrosothiol mediated by nitrosonium (Scheme 1). In this process, nitrosonium binds nitrosothiol, leading to a stable electrophilic complex that reacts with a second equivalent of nitrosothiol, releasing the nitric oxide dimer and nitrosated disulfide. This latter species acts as a powerful source of nitrosonium, completing the catalytic cycle. The proposed mechanism has been tested by evaluation of the decomposition of *S*-nitroso-*n*-hexylthiol in the presence of various sources of nitrosonium.

Scheme 1. Proposed Cationic Catalytic Cycle for Decomposition of RSNO (R = Me)

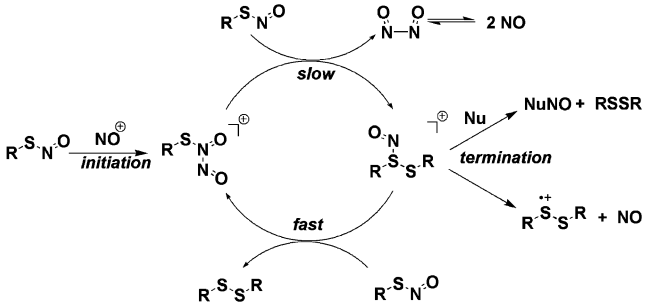

Results and Discussion

Nitrosation of *S*-Nitrosothiol. In the gas phase, nitrosonium can nitrosate both *cis*- and *trans*-*S*-nitrosomethanethiol on either nitrogen or sulfur to form the novel cation−molecule species *N*-nitrosonium-*S*-nitrosomethanethiol (**4**−**7**) and *S*-nitrosonium-*S*-nitrosomethanethiol (**8**−**10**) (Figure 1). Formation of these complexes is barrierless and exothermic by 24 to 34 kcal mol^{-1} in the gas phase. The C−S−N−O functionality is essentially planar, with dihedral angles near 0° (cis) or 180° (trans). Five of the complexes (**4**−**6**, **8**, **10**) are C_s symmetric; the O−N−N−O dihedral angle in cation **7** is 139°, and cation **9** has two different *cis*- and *trans*-NO substituents. The S−N bond lengths of the *N*-nitrosonium-*S*-nitrosomethanethiols (**4**−**7**) range from 1.68 to 1.73 Å. The nitrosonium moiety is bound only loosely, and the positive charge is borne partially by the sulfur atom. In contrast to the S−N bonds of *N*-nitrosonium-*S*-nitrosomethanethiols, the S−N bonds of the *S*-nitrosated species are elongated by 0.4 Å, with two NO groups bound loosely to sulfur. A similar lengthening of the S−N bond (0.25 Å) has been reported in calculations of a Cu^{I}−nitrosothiol complex.[9] The lowest energy conformer of the dinitrosothiol cation is the *cis*,*cis*-*N*-nitrosonium-*S*-nitrosothiol species **4** with a N−N distance of 2.14 Å. The isomeric complexes **5**−**10** show energies 3.1, 4.9, 10.2, 1.4, 1.8, and 2.8 kcal mol^{-1} above that of **4**, respectively, in the gas phase. The preference for the *cis*-C−S−N−O dihedral arises from repulsion between lone pairs on oxygen and sulfur. A similar preference was previously noted in a study of anionic nitroxyl disulfide.[10]

Both **4** and **8**, the two lowest-energy structures of the *N*- and *S*-nitrosated species, exist as resonance hybrids (Scheme 2). Mulliken charges on **4** indicate that half of the positive charge is borne by the sulfur atom and the remaining half by the appended NO group. The central NO moiety bears essentially no charge. In the symmetrical structure, **8**, the largest portion of the charge (32%) is borne by the sulfur, with the remaining charge distributed between the nitrogens (23%) and oxygens (11%) of the equivalent NO moieties.

Scheme 2. Canonical Contributors to *N*- and *S*-Nitrosonitrosothiol Resonance Hybrids

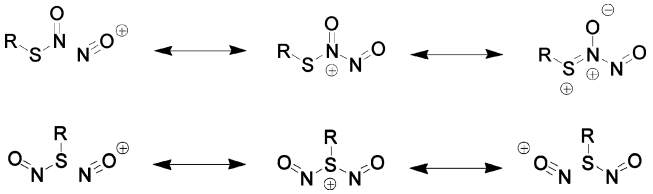

The energetics of the nitrosation of *S*-nitrosothiol by various nitrosating agents are shown in Table 1. For ionic NO^+ donors, such as $NO^+ \cdot BF_4^-$, $NO^+ \cdot PCl_6^-$, and $NO^+ \cdot SbCl_6^-$, the addition of NO^+ to RSNO is thermodynamically favorable. Since solvation energies of NO^+ are greater than that of [RS(NO)-NO^+], the free energy of reaction becomes less favorable as solvent polarity increases: ΔG_{rxn} for the nitrosation of MeSNO increases from −24 kcal mol^{-1} in the gas phase to −10 kcal mol^{-1} in acetonitrile. Although NO^+ has only a fleeting existence in water because of rapid hydrolysis ($NO^+ + 2H_2O \rightarrow HNO_2 + H_3O^+$), the dinitrosothiol cation, [RS(NO)NO^+], could survive in methanol, acetonitrile, and *n*-heptane solutions even with traces of water (Table 1).[11] Nitrosation by weaker sources of nitrosonium, such as O_2 + NO, N_2O_3, N_2O_4, CH_3-ONO, or CH_3SNO, is considerably less favorable than by nitrosonium salts, and nitrosations by alkyl nitrite or nitrosothiol are predicted to be endothermic.

Nitric oxide and dioxygen, when dioxygen is present in a considerable concentration, can react rapidly to form various oxides of nitrogen, in particular N_2O_3 and N_2O_4.[12,13] Grossi and co-workers have proposed a mechanism of nitrosothiol decomposition that involves a one-electron oxidation of RSNO by N_2O_3 to generate the corresponding nitrosothiol radical cation.[8] Our calculations suggest this reaction is highly unfavorable, with a $\Delta G_{rxn,gas}$ of 164 kcal mol^{-1}. The reaction is somewhat less unfavorable in polar solvents, with predicted free energies of 99 kcal mol^{-1} and 31 kcal mol^{-1} in *n*-heptane and acetonitrile, respectively. These calculated values are for the reaction of separated ions, and reaction through ionic pairs could further lower these endothermicities. In contrast, the radical recombination of RSNO$^{\bullet+}$ with NO to form [RS(NO)NO^+] (R = Me) is quite exothermic with ΔG_{rxn} values of −20, −18, and −16 kcal mol^{-1} in the gas phase, *n*-heptane, and acetonitrile, respectively (Table 1). Together, these calculations strongly suggest that the reaction of RSNO with N_2O_3 is more likely to produce [RS-(NO)NO^+] than RSNO$^{\bullet+}$.

(8) (a) Grossi, L.; Montevecchi, C.; Strazzari, S. *J. Am. Chem. Soc.* **2001**, *123*, 4853−4854. (b) Lipton, S. A.; Choi, Y. B.; Pan, Z. H.; Lei, S. Z.; Chen, H. S.; Sucher, N. J.; Loscalzo, J.; Singel, D. J.; Stamler, J. S. *Nature* **1993**, *364*, 626−632.
(9) Toubin C.; Yeung, D. Y. H.; English, A. M.; Peslherbe, G. H. *J. Am. Chem. Soc.* **2002**, *124*, 14816−14817.
(10) Houk, K. N.; Hietbrink, B. N.; Bartberger, M. D.; McCarren, P. R.; Choi, B. Y.; Voyksner, R. D.; Stamler, J. S.; Toone, E. J. *J. Am. Chem. Soc.* **2003**, *125*, 6972−6976.
(11) MeS═NOH$^+$ is a higher-energy isomer of MeSH(NO)$^+$; at the B3LYP/6-31+G* level, the former is higher by 1.7 kcal/mol than the latter.
(12) Olson, L. P.; Kuwata, K. T.; Bartberger, M. D.; Houk, K. N. *J. Am. Chem. Soc.* **2002**, *124*, 9469−9475.
(13) Grossi, L.; Strazzari, S. *J. Org. Chem.* **1999**, *64*, 8076−8079 and references therein.

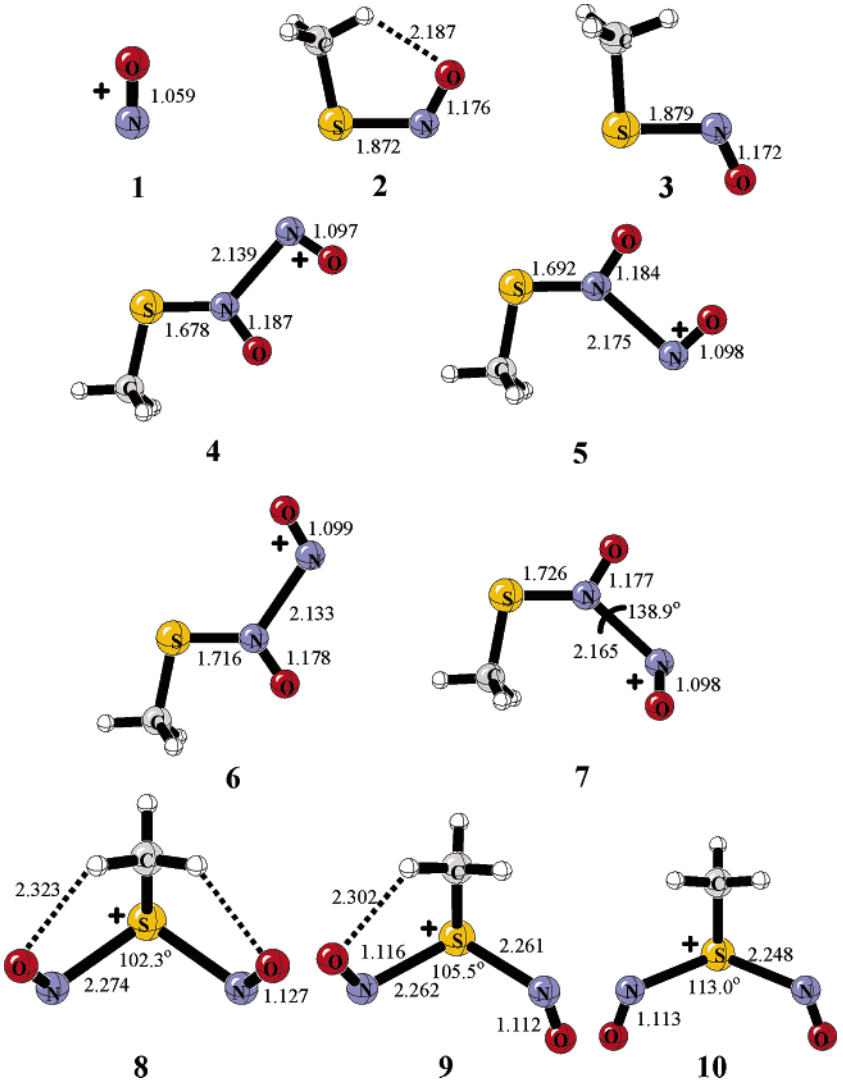

Figure 1. Calculated structures for secondary nitrosation of RSNO with the CBS-QB3 method.

Table 1. Calculated Free Energies ($\Delta G_{298,rxn}$ in kcal/mol) of Reactions of RSNO with NO^+ or Other Donors

		CBS-QB3	(CPCM)//B3LYP/CBSB7
entry	reaction	gas phase	acetonitrile
1	$NO^+ + MeSNO \rightarrow MeS(NO)NO^+$	−24.2	−10.2
2	$NO^+ + 2H_2O \rightarrow HNO_2 + H_3O^+$	+13.0	−0.2
3	$MeS(NO)NO^+ + MeOH \rightarrow MeS(H)NO^+ + MeONO$	+8.7	+6.7
4	$MeS(NO)NO^+ + H_2O \rightarrow MeS(H)NO^+ + HONO$	+14.7	+11.8
5	$MeS(NO)NO^+ + 2H_2O \rightarrow MeSNO + HONO + H_3O^+$	+37.2	+10.0
6	$MeS(NO)NO^+ + MeSH \rightarrow MeS(H)NO^+ + MeSNO$	+1.3	−1.6
7	$4\ NO + O_2 \rightarrow 2N_2O_3$	−15.8	−22.8
8	$2\ NO + O_2 \rightarrow N_2O_4$	−20.6	−24.1
9	$N_2O_3 + MeSNO \rightarrow MeS(NO)NO^+ + NO_2^-$	+136.9	−5.3
10	$N_2O_4 + MeSNO \rightarrow MeS(NO)NO^+ + NO_3^-$	+125.1	−12.9
11	$MeONO + MeSNO \rightarrow MeS(NO)NO^+ + MeO^-$	+182.9	+37.8
12	$2\ MeSNO \rightarrow MeS(NO)NO^+ + MeS^-$	+168.7	+34.7
13	$N_2O_3 + MeSNO \rightarrow MeSNO^{\bullet+} + N_2O_3^{\bullet-}$	+163.9	+31.3
14	$MeSNO^{\bullet+} + NO \rightarrow MeS(NO)NO^+$	−20.1	−16.4
15	$MeSSMe(NO)^+ \rightarrow MeSSMe + NO^+$	+28.8	+7.7
16	$MeSSMe(NO)^+ \rightarrow MeSSMe^{\bullet+} + NO$	−1.1	+0.8
17	$MeSSMe + MeSSMe(NO)^+ \rightarrow (MeSSMe)_2(NO)^+$	−8.0	+9.7

Disulfide Formation from RSNO + [RS(NO)NO$^+$]. The sulfur of nitrosated nitrosothiol is strongly electrophilic, and a displacement reaction with RSNO produces a nitrosated disulfide and the NO dimer. Sixteen transition states were located for the S_N2 reaction of *N*- and *S*-nitrosonium-nitrosothiols with RSNO using B3LYP/6-31+G* and B3LYP/CBSB7 methods (see Supporting Information). All of the *N*-nitrosonium-*S*-nitrosothiol transition states are lower in energy than the corresponding *S*-nitrosonium-*S*-nitrosothiols. The two rotameric lowest-energy transition states (**11**, **12**) were studied further with

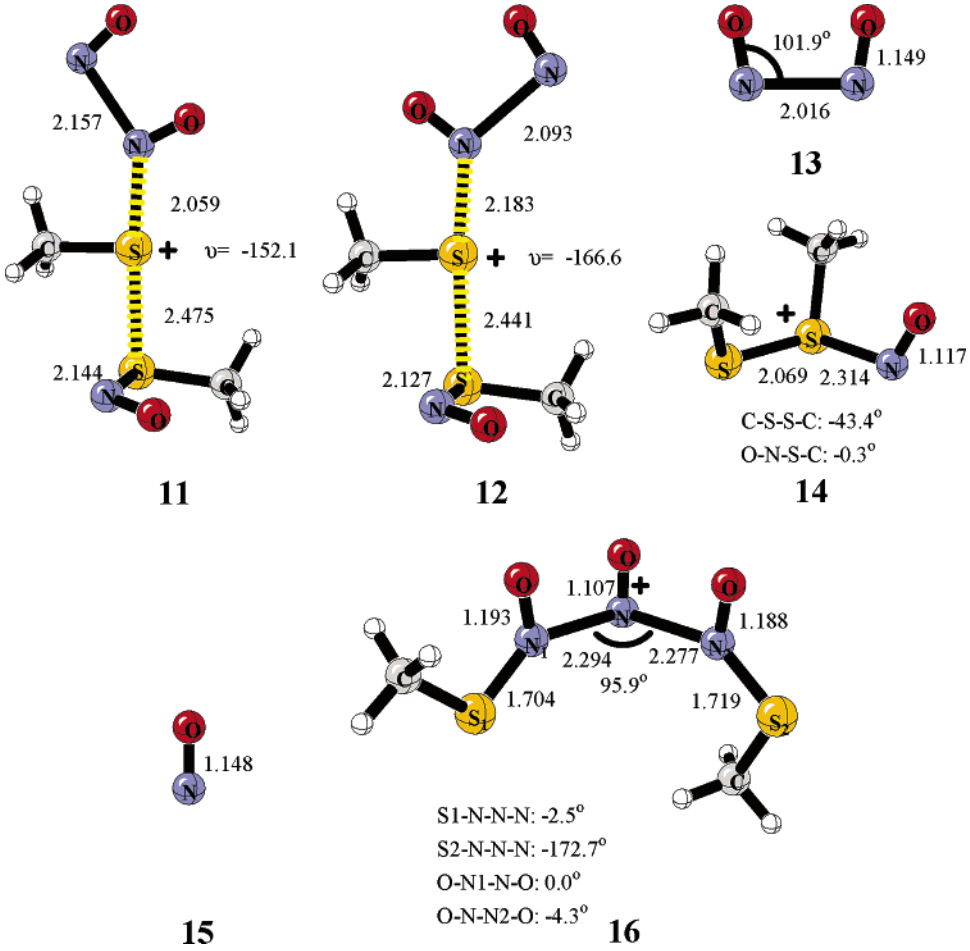

Figure 2. Calculated structures of the transition states and products for S_N2-like S−S forming reaction with the CBS-QB3 method.

CBS-QB3 calculations (Figure 2). Both transition states show typical S_N2 characteristics: a nearly linear N−S−S arrangement, a lengthened N−S bond (2.06 Å; 2.18 Å), and a forming S−S bond (2.48 Å; 2.44 Å). The relative gas-phase energies of the two transition states are 7.9 and 9.4 kcal mol^{-1}, respectively (CBS-QB3).[14]

All transition states resulting from nitrosothiol attack on *N*-nitrosonium-*S*-nitrosothiol lead to identical products: the NO dimer and a nitrosonium disulfide cation (**14**, Figure 2). The novel cation has a normal S−S bond length of 2.07 Å and an elongated S−N bond length of 2.32 Å, consistent with a nitrosonium ion weakly coordinated to disulfide. Frequency analysis confirms that this structure is a true energy minimum bound by 38 kcal mol^{-1} (enthalpy) relative to CH_3SSCH_3 + NO^+ in the gas phase (Table 1). The 1.12 Å N−O bond length of **14** is consistent with N−O bonds of *S*-dinitrosothiols, but it is somewhat longer than the 1.06 Å length calculated for NO^+ at the same theory level. Rapid dissociation of the NO dimer into monomer provides a driving force for the overall reaction.

The lowest enthalpy reaction pathway passes through transition state **11**, with a gas-phase activation enthalpy of 7.9 kcal mol^{-1} above complex **16** and 4.9 kcal mol^{-1} below dissociated RSNO and $RS(NO)NO^+$ (CBS-QB3). This barrier is significantly lower than that for homolytic scission of nitrosothiol to free NO and the thiyl radical which, at 27 kcal mol^{-1}, makes this decomposition manifold of only minor importance near physiologically relevant temperatures.[15] The activation free energy for nucleophilic displacement of NO dimer from *N*-nitrosonium-*S*-nitrosothiol by nitrosothiol is 8 kcal mol^{-1}, reflecting the entropy loss during bimolecular reaction. Both the reactive complex and the transition state are solvated less effectively than are the isolated reactants. As a result, the activation free energies ($\Delta G_{sol}^{\ddagger}$) increase by 4 and 10 kcal mol^{-1} in *n*-heptane and acetonitrile, respectively (Figure 3). Nonetheless, the overall resulting free energy of activation in acetonitrile (18 kcal mol^{-1}) is still significantly more favorable than homolytic scission of the nitrosothiol S−N bond.

Nitrosonium Transfer. Completion of the catalytic cycle requires transfer of a nitrosonium equivalent from the nitrosated disulfide. While this process is predicted to be endothermic by 4 kcal mol^{-1} in the gas phase, the same process is calculated to be exothermic by 2 kcal mol^{-1} in acetonitrile solution, due to differential solvation of the *N*-nitrosonium-*S*-nitrosothiol (Figure 4).

Transfer could conceivably proceed via either an associative (addition/elimination) or a dissociative pathway. Dissociation

(14) The intramolecular transition state for rotation around the S−N bond can interconvert **4** and **5** (see Supporting Information). The activation free energies are +20.4 and +18.1 kcal/mol in gas phase and acetonitrile, respectively.

(15) The activation energy of 27 kcal/mol is the free-energy maxima in the homolysis of RSNO. We also located a concerted bimolecular transition structure with a barrier of 36 kcal/mol ($\Delta H^{\ddagger}$) and 45 kcal/mol ($\Delta G^{\ddagger}$) in the gas phase.

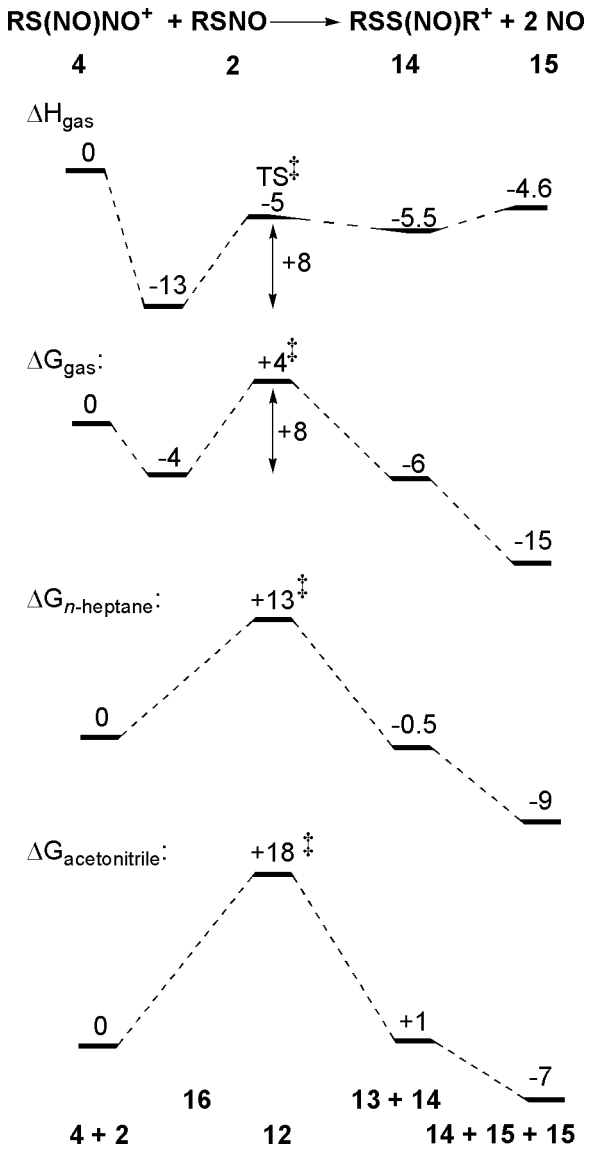

Figure 3. Energetic profile of the S_N2 reaction between $RS(NO)NO^+$ and RSNO (R = Me).

of nitrosonium from the nitrosodisulfide cation is endothermic by 29, 17, and 8 kcal mol^{-1} in the gas phase, *n*-heptane, and acetonitrile, respectively. The association free energies (ΔG_{assn}) for $RSS(NO)R^+$ and RSNO into complex $[RSSR(NO)RSNO]^+$ (**17**, Figure 5) are −4, 3, and 8 kcal/mol in the gas phase, *n*-heptane ($\epsilon = 1.92$), and acetonitrile ($\epsilon = 36.64$), respectively (CBS-QB3, CPCM). Overall, an associative pathway is the strongly preferred route for nitrosonium transfer in low polarity solvents, while the dissociative mechanism becomes competitive in polar solvents.

The associative mechanism of nitrosonium transfer passes through intermediate **17**. The calculated gas-phase structure of this intermediate shows a central N−S distance of 2.48 Å and a N−N bond length of 2.29 Å. The S−N bond of the RSNO moiety is slightly shortened from 1.87 Å to 1.71 Å, similar to that observed in *N*-nitrosonium-*S*-nitrosothiol. To confirm that **17** is a true minimum in solution, the structure was reoptimized in acetonitrile ($\epsilon = 36.64$) at the B3LYP/6-31+G* level. The reoptimized structure is virtually identical to that derived in gas-phase calculations.[16]

Isomerization between 4 and 5. The initial *N*-nitrosated-*S*-nitrosothiol cation exists as an equilibrating mixture of rotamers

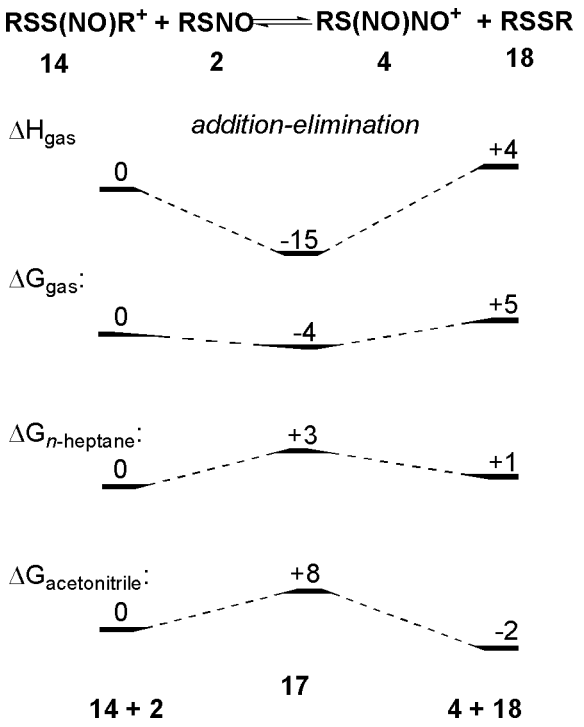

Figure 4. Energetic profile for nitrosonium transfer.

(**4** and **5**). Conceptually, the simplest interconversion of the isomers involves rotation around the S−N bond. This process, however, shows an activation barrier of roughly 20 kcal mol^{-1} both in the gas phase and in solvents of all polarities. Nitrosonium transfer by addition−elimination offers an alternative process for isomerization and is likely important at high nitrosothiol concentrations.[17] The intermediate in this transfer (**16**, Figure 2) is formed in a barrierless process that is exothermic in the gas phase (−4.5 kcal mol^{-1}) and slightly endothermic in the condensed phase (4 and 9 kcal mol^{-1} in hexane and acetonitrile, respectively). The unusual cation, which formally bonds three NO equivalents, places two *N*-nitrosonium-*S*-nitrosothiol planes in an almost orthogonal orientation, with a N−N−N angle of about 96°. As was the case for the nitrosodisulfide cation, a dissociative mechanism proceeding through free nitrosonium is significantly more endothermic than the associative route: dissociation of **4** to NO^+ is endothermic by 24, 17, and 10 kcal mol^{-1} in the gas phase, *n*-heptane, and acetonitrile, respectively.

Termination of the NO^+-Catalyzed RSNO Decomposition: The chain mechanism proposed here effectively relies on nitrosonium as the chain-carrying species: any species that scavenges nitrosonium will terminate the chain. Such species include oxygen and sulfur nucleophiles, and a nitrosonium-scavenging chain-termination mechanism is consistent with the well-known stabilizing effect of excess thiol. Dissociation of the nitrosodisulfide cation to neutral NO and the disulfide radical cation also terminates chains. The reaction is endothermic by 10 kcal mol^{-1} but has a favorable free energy.[18] The resulting disulfide radical cation populates a planar structure (C−S−S−

(16) Because of the flatness of the potential energy surface, no transition state is located for breaking and forming intermediates **16** and **17**. The estimated activation energy, even in acetonitrile, is less than 3 kcal/mol with respect to the intermediate based on scanning calculations.

(17) The energetic profiles of the elimination−addition, addition−elimination, and intramolecular rotation mechanisms for the isomerization between **4** and **5** are shown in the Supporting Information.

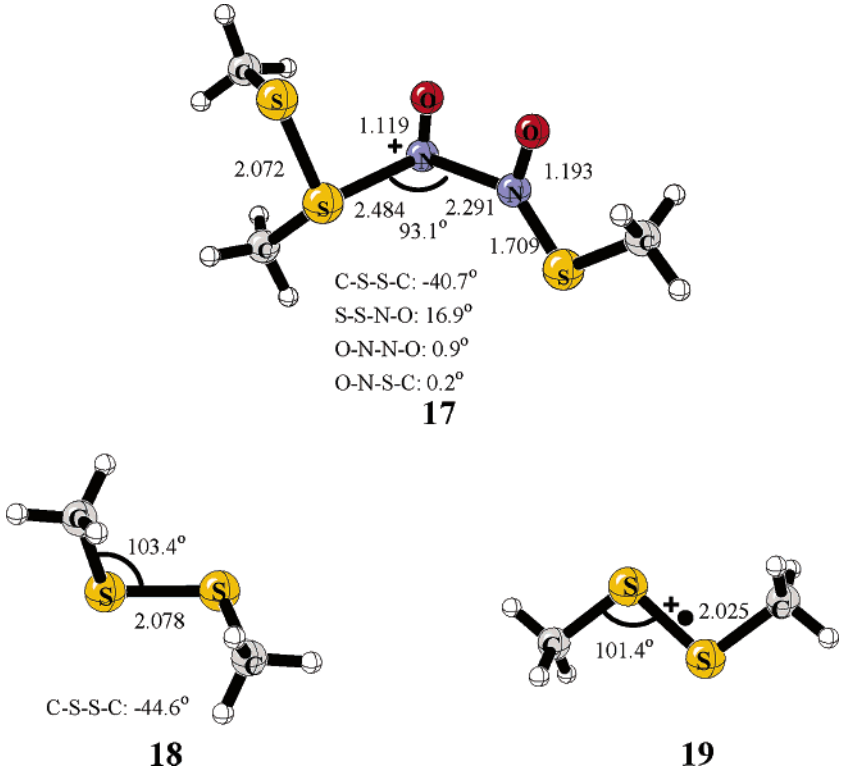

Figure 5. Calculated structure of disulfide, nitrosothiol-coordinated nitrosonium with the CBS-QB3 method.

C: 180°), in contrast to the neutral disulfide which adopts the typical C−S−S−C dihedral of ±90°.[19] The radical cation also shows a slightly shorter S−S bond (0.05 Å) than the neutral disulfide.

Experimental Study of NO^+-Catalyzed Decomposition: The stability of *n*-hexyl nitrosothiol was examined in the presence of various sources of nitrosonium. As suggested by calculations, nitrosothiol decomposition is initiated catalytically by strong sources of nitrosonium ($NOBF_4$, $NOPF_6$), but not by alkyl nitrites. In the absence of NO^+, a 25 mM solution of C_6H_{13}-SNO in degassed acetonitrile decomposes only very slowly at room temperature (Figure 6a). The addition of 2 mM (8 mol %) $NOBF_4$ to a sealed reaction vessel resulted in a rapid initial decomposition: roughly half of RSNO is lost in 20 min. The reaction does not, however, proceed to completion, and following this initial burst, further decomposition proceeds at a rate roughly equivalent to that observed in the absence of nitrosonium catalyst. The chain reaction proposed in Scheme 1 predicts that excess neutral nitric oxide will ultimately inhibit nitrosothiol decomposition. In good agreement with this mechanism, a similar reaction continually sparged with helium to remove NO results in clean and complete decomposition (Figure 6c). The time course of the decomposition was modeled according to the catalytic decomposition mechanism of Scheme 1 using the REACT software. Eyring theory predicts second-order rate constants of 0.40 M^{-1} s^{-1} and 8.5×10^6 M^{-1} s^{-1} for displacement of the NO dimer from nitrosated nitrosothiol and nitrosation of nitrosothiol by nitrosated disulfide, given calculated activation free energies of 18 and 8 kcal mol^{-1}, respectively. The calculated and observed decomposition profiles show remarkable agreement (Figure 6).

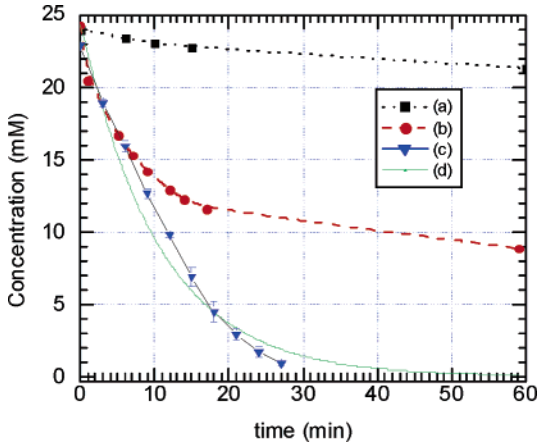

Figure 6. Kinetics of nitrosonium-catalyzed decomposition of RSNO (R: hexyl, 25 mM) in degassed acetonitrile: (a) in the absence of NO^+, (b) in the presence of 2 mM $NOBF_4$, no special effort to remove NO during the decomposition, (c) 2 mM $NOBF_4$, continually sparging to remove NO, and (d) in the presence of 2 mM NO^+, using simulation program (REACT), based on the current mechanism (Figure 6). Note: the difference between (c) and (d) may be due to monitor-starting-time error.

The rate-determining step of the catalytic decomposition is the nucleophilic displacement of the NO dimer from the cationic nitrosated nitrosothiol. The activation barrier for this conversion via an associative mechanism is calculated to be solvent-dependent, with the rate of reaction diminishing with increasing solvent polarity. To test this hypothesis, the decomposition of *n*-hexyl nitrosothiol was initiated with 8 mol % $NOBF_4$ in toluene ($\epsilon = 2.38$), chloroform ($\epsilon = 4.81$), and acetonitrile ($\epsilon = 36.7$). In contrast to the predicted solvent effect, rates of decomposition *increase* with increasing solvent polarity (Figure

(18) Attempts to achieve the diradicaloid transition state failed for the monotonic uphill potential surface. The estimated barrier for decomposition should be slightly lower than the reaction enthalpy of 10 kcal/mol because of favorable entropy changes.
(19) *cis*-$RSSR^{\bullet+}$ (R = Me) is slightly higher energy than *trans*- (see Supporting Information).

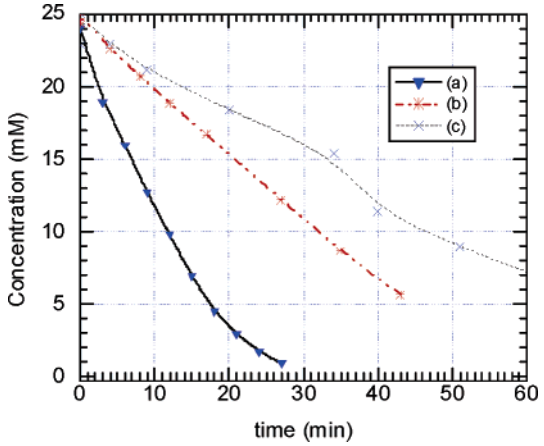

Figure 7. Solvent effects on *n*-hexylnitrosothiol decomposition, in the presence of 2 mM $NOBF_4$, continually sparging to remove NO: (a) in degassed acetonitrile, (b) in chloroform−acetonitrile mixed solvent (v:v = 14:1), (c) in toluene−acetonitrile mixed solvent (v:v = 14:1). Note: in (b) and (c), add stock $NOBF_4$/acetonitrile solution into chloroform and toluene solutions of nitrosothiol, respectively.

7). This observation is likely the result of opposing solvent effects on the two chain steps. On one hand, the rate-determining nucleophilic displacement of the NO dimer from nitrosated nitrosothiol should be enhanced in low-polarity solvents, predicting a diminishing rate of reaction over the series toluene, chloroform, and acetonitrile. On the other hand, nitrosonium transfer from nitrosated disulfide to nitrosothiol is enhanced in polar solvent, raising the concentration of the key *N*-nitroso-*S*-nitrosothiol intermediate. These two effects apparently very nearly cancel, resulting in similar rates of decomposition across the solvent spectrum. Additionally, stable solvent complexes may account for deviations from the solvent predicted dependence. Such complexes have been observed in other aromatic solvents and are presumably important during the toluene decomposition reaction. Finally, all calculations were conducted only for the methyl-substituted thiol; corresponding values for other nitrosothiols may vary slightly. The most significant changes upon going from our MeSNO model system to biological RSNOs are expected to stem from varying solvation energy contributions depending on the substituents.

Conclusion

Despite the phenomenologically well described decomposition of nitrosothiols to nitric oxide and disulfide, a plausible molecular mechanism for this transformation under oxidative conditions is lacking. Here, we have proposed a nitrosonium-catalyzed process with both a predicted and an experimental free energy of activation of roughly 18 kcal mol^{-1}. The proposed mechanism rationalizes at least some of the phenomenology of nitrosothiol spontaneous decomposition:

- The scavenging effect of free reduced thiol on the nitrosonium catalyst is consistent with the observation that thiol stabilizes nitrosothiol solutions.
- The proposed mechanism is strongly dependent on nitrosothiol concentration, in keeping with the general observation that nitrosothiols are less stable in concentrated solution.
- The reaction is dependent on the ratio of concentrations of nitrosothiol, disulfide, nitric oxide, and nitrosonium present in the solution, consistent with the frequent observation of non-integral rate laws for decomposition.
- At least one of the potentially rate-determining steps involves a sterically congested nucleophilic displacement reaction, consistent with the general observation that tertiary nitrosothiols are more stable than their primary and secondary counterparts.
- Many nitrosothiols show strongly diminished stabilities at low pH; such conditions could favor the proteolytic release of nitrosonium, inducing catalytic decomposition.

The chemistry of nitrosothiols is rich and complex, and the mechanism of nitrosothiol decomposition is almost certainly highly dependent on reaction conditions. The catalytic pathway proposed here likely competes with unimolecular homolytic cleavage and other catalyzed decomposition mechanisms, including metal-catalyzed and photolytic processes.

Computational Methodology

Quantum mechanical calculations were carried out with density functional theory using the B3LYP density functional theory and the 6-31+G* basis set[20] in Gaussian98 and Gaussian03.[21] All stationary points were verified by harmonic vibrational frequency analysis at the B3LYP level. These stationary points were reoptimized using the CBS-QB3 method by Petersson et al.,[22] known to have a mean error of 1 kcal mol^{-1} for the G2 experimental data set. The free energies in solvent shown were calculated at the B3LYP/CBSB7 level using CPCM with Pauling-(Merz−Kollman) atomic radii[9] and added to the gas-phase CBS-QB3 energies. All free energies are given for 298 K, 1 M concentrations for solution phase results and at 1 atm pressure for gas-phase calculations.

Kinetics of Nitrosonium-Catalyzed Decomposition of RSNOs: All reagents (acetonitrile, chloroform, toluene, 1-hexanethiol, *tert*-butylnitrite, $NOBF_4$) were purchased from Aldrich Chemical Co. and used without further purification. *S*-Nitroso-*n*-hexanethiol was prepared in situ by nitrosation of *n*-hexanethiol with *tert*-butylnitrite.

Kinetic studies were performed using an HP 8453 UV−vis spectrophotometer. All reagents and solutions were transferred with gastight syringes. Solvents were rigorously degassed either by sparging (He) or by freeze/thaw. The time courses of reactions were followed by monitoring the disappearance of RSNO absorbance at either 550 or 551 nm. A background correction was made by subtracting the absorbance at 700 or 800 nm. Sparging experiments were done in 100-mL round-bottom flasks, while sealed experiments were done in 3.5-mL screw-top cuvettes lined with PTFE-rubber septa.

In a typical sparging experiment, a flask was fitted with stir bar and rubber septum and then flushed with N_2. Solvent was added, followed by 1-hexanethiol and TBN, and sparging (He) was initiated. An initial absorption reading was taken, followed by addition of $NOBF_4$ stock. At various time points, 1-mL aliquots of the reaction mixture were removed from the flask for UV−vis analysis.

In a typical sealed experiment, a 3.5-mL screw-top cuvette was flushed with N_2. Solvent was added, followed by 1-hexanethiol and TBN. An initial UV−vis absorption reading was taken, followed by addition of $NOBF_4$ stock. At various time points, absorptions were recorded using the same cuvette.

Curve Simulation. The *REACT for Windows* simulation program was downloaded free of charge from Alchemy Software (http://chemicalsoft.com/). Rate constants for the two propagation steps were derived by Eyring analysis using calculated free energies of activation. The initial RSNO concentration was set at 25 mM, and the initial RS-(NO)NO^+ concentration was set at 2 mM.

(20) Becke, A. D. *J. Chem. Phys.* **1993**, *98*, 5648−5652.
(21) Frisch, M. J. et al. *Gaussian 98 and 03*; Gaussian, Inc., Pittsburgh, PA.
(22) Montgomery, J. A.; Frisch, M. J.; Ochterski, J. W.; Petersson, G. A. *J. Chem. Phys.* **1999**, *110*, 2822−2827. (U)B3LYP/6-31+G*, (U)B3LYP/CBSQB7, and CBS-QB3 methods result in similar energetic patterns for the NO^+-catalyzed mechanism; the DFT methods underestimated BDE and activation energy by 2−3 kcal mol^{-1}, comparing to CBS-QB3, which has been shown to work well for similar species previously.

Acknowledgment. We are grateful to the National Institute of General Medical Sciences, National Institutes of Health, for financial support of this research.

Note Added after ASAP Publication. After this article was published ASAP on July 15, 2005, a typographical error occurring in both Figures 3 and 4 was corrected. The corrected version was published ASAP on July 19, 2005.

Supporting Information Available: Optimized structures and energies for all species discussed, the 16 S_N2 transition states using the B3LYP/6-31+G* and B3LYP/CBSB7 methods, the intramolecular rotation transition state for conversion between **4** and **5**, the experimental *n*-C_3H_7SNO decay time in different solutions, and complete ref 21 (PDF). This material is available free of charge via the Internet at http://pubs.acs.org.

JA050018F